

Electronic and Magnetic Circular Dichroism Spectra of Linear Two-Coordinate Gold(I) Complexes of Alkyl Isocyanide or Trialkyl Phosphite Ligands

STEVEN K. CHASTAIN and W. ROY MASON*

Received February 8, 1982

Absorption and magnetic circular dichroism (MCD) spectra are reported for $[\text{Au}(\text{CNEt})_2]\text{ClO}_4$, $\text{Au}(\text{CN})(\text{CNMe})$, and $[\text{Au}(\text{P}(\text{OMe})_3)_2]\text{ClO}_4$ in acetonitrile solution at room temperature. Each complex exhibits several intense bands in the ultraviolet region, which are assigned to metal-to-ligand charge transfer (MLCT) from the filled Au(I) 5d molecular orbitals to the lowest energy empty orbital $2\pi_u$, which is predominantly ligand based. The spectra for $\text{Au}(\text{CNEt})_2^+$ are interpreted in detail by means of a model that includes gold spin-orbit coupling in the excited MLCT states. Relative magnitudes of the MCD terms are calculated for $\text{Au}(\text{CNEt})_2^+$ and compared with experimental spectra. The lowest energy band in all three complexes is shown to exhibit a pseudo A term comprised of B terms of opposite sign for the Σ_u^+ and Π_u spin-orbit states derived principally from the $a^3\Pi_u$ state of the $(2\sigma_g^+)(2\pi_u)$ excited configuration. The participation of the Au(I) orbitals in metal-to-ligand π bonding and σ bonding is discussed.

Introduction

The experimental investigation of the electronic structure of linear two-coordination has focused on gold(I) complexes quite naturally because of their variety, stability, and resistance to ligand addition and increased coordination. Consequently the electronic spectra of representative Au(I) complexes continue to be of interest.^{1,2} Among the more interesting examples that have been studied in detail has been the $\text{Au}(\text{CN})_2^-$ ion.^{2,3} This ion exhibits rich, structured spectra in the UV region which has been assigned to metal-to-ligand charge transfer (MLCT) from filled 5d orbitals of Au(I) to empty, primarily ligand-based π^* orbitals of the π -acceptor CN^- ligands. Much of the understanding of the MLCT process as it operates in two-coordinate complexes rests on the interpretation of the spectra of this ion. Unfortunately, there have been few electronic spectral studies of other Au(I) complexes containing π -acceptor ligands;^{4,5} this has been partly due in many cases to the presence of strong ligand absorptions which obscure MLCT transitions of the complex as a whole. Motivated in part by our general interest in the MLCT process and the desire to advance the understanding of electronic structure of linear two-coordination and to characterize low-energy excited states in gold(I) complexes, we have expanded our investigation to some other π -acceptor ligands. We report here absorption and magnetic circular dichroism (MCD) spectra for $\text{Au}(\text{CNEt})_2^+$, $\text{Au}(\text{CNMe})(\text{CN})$, and $[\text{Au}(\text{P}(\text{OMe})_3)_2]^+$. The CNR ligands have empty π^* orbitals analogous to the acceptor orbitals of CN^- , while the acceptor orbitals of $\text{P}(\text{OMe})_3$ are the 3d orbitals of the P donor. The CN^- , CNR, and $\text{P}(\text{OMe})_3$ ligands are all virtually transparent in the UV region, allowing molecular transitions of the complex to be observed.

Experimental Section

Preparation of Compounds. Bis(ethyl isocyanide)gold(I) perchlorate, $[\text{Au}(\text{CNEt})_2]\text{ClO}_4$, and bis(trimethyl phosphite)gold(I) perchlorate, $[\text{Au}(\text{P}(\text{OMe})_3)_2]\text{ClO}_4$, were both prepared under a dry-nitrogen atmosphere from solid bis(acetonitrile)gold(I) perchlorate, $[\text{Au}(\text{CH}_3\text{CN})_2]\text{ClO}_4$,⁶ and solutions containing excess ligand. For $[\text{Au}(\text{CNEt})_2]\text{ClO}_4$, $[\text{Au}(\text{CH}_3\text{CN})_2]\text{ClO}_4$ was treated with ethyl isocyanide⁷ dissolved in a 1:10 $\text{CH}_3\text{CN}-\text{CCl}_4$ solution. When a 1:1

mixture of cyclohexane-ether was added to the resulting solution, an oily layer separated, which was dissolved in acetone. The product was precipitated by adding ether and cooling in a dry ice-acetone bath. The solid was collected and reprecipitated from acetone with ether at dry ice temperature. For $[\text{Au}(\text{P}(\text{OMe})_3)_2]\text{ClO}_4$, $[\text{Au}(\text{C}-\text{H}_3\text{CN})_2]\text{ClO}_4$ was suspended in CHCl_3 and redistilled trimethyl phosphite (Strem Chemical Co.) was added dropwise until a solution resulted. The product was precipitated by adding ether and reprecipitated from CH_3Cl with ether. Both compounds gave satisfactory elemental analyses for two-coordinate complexes. $[\text{Au}(\text{CN})(\text{CNMe})]$ was prepared from $[(n-\text{C}_4\text{H}_9)_4\text{N}][\text{Au}(\text{CN})_2]^3$ and methyl iodide according to a literature method.⁸ Satisfactory elemental analyses were also obtained for this compound.

Attempts made to prepare bis(ethyl isocyanide)mercury(II) perchlorate, $[\text{Hg}(\text{CNEt})_2](\text{ClO}_4)_2$, and bis(trimethyl phosphite)mercury(II) perchlorate, $[\text{Hg}(\text{P}(\text{OMe})_3)_2](\text{ClO}_4)_2$, from $\text{Hg}(\text{ClO}_4)_2 \cdot 3\text{H}_2\text{O}$ suspended in CCl_4 by adding the ligands dropwise resulted in solutions from which unstable solid compounds were precipitated on the addition of ether. Acetonitrile solutions of these compounds were stable for several hours but showed no absorption maxima or shoulders below $5.2 \mu\text{m}^{-1}$. The solids rapidly decomposed at room temperature. **Caution:** the solid formed from $\text{P}(\text{OMe})_3$, presumably $[\text{Hg}(\text{P}(\text{OMe})_3)_2](\text{ClO}_4)_2$, detonated on collection. No further attempts were made to purify or characterize this compound.

Spectral Measurements. Absorption measurements were made using a Cary Model 1501, while MCD spectra were recorded on a JASCO ORD/UV-5 (equipped with a CD attachment) using a permanent magnet (field 1.0 T). Spectroquality acetonitrile was used throughout for solution spectra. Measurements were all made at room temperature. Solutions were found to be stable for several days when stored in the dark. No changes in the spectra were noted over the time required for the measurements.

Computations. Spin-orbit eigenvalues and eigenvectors for allowed Π_u and Σ_u^+ MLCT excited states for $\text{Au}(\text{CNEt})_2^+$ were computed by diagonalization of appropriate Π_u and Σ_u^+ secular determinants which have been given previously.^{2,9} Input values for the calculations consisted of energies for the singlet and triplet states of the $2\pi_u$ MLCT excited configurations in the absence of spin-orbit coupling, together with ζ_{5d} for Au(I) (taken to be $0.30 \mu\text{m}^{-1}$). Calculated eigenvalues were compared with the experimental absorption spectra for $\text{Au}(\text{CNEt})_2^+$, and the input values were chosen to give the best agreement. The choices of input values were further constrained since the eigenvectors were used to compute MCD A and B terms. A wide range of input parameters was used, and those significantly different from the final reported values failed to give good agreement between the calculated energies and A and B terms with the observed absorption and MCD spectra.

(1) Koutek, M. E.; Mason, W. R. *Inorg. Chem.* **1980**, *19*, 648.(2) Mason, W. R. *J. Am. Chem. Soc.* **1976**, *98*, 5182.(3) Mason, W. R. *J. Am. Chem. Soc.* **1973**, *95*, 3573.(4) Fenske, G. P.; Mason, W. R. *Inorg. Chem.* **1974**, *13*, 1783.(5) Brown, D. H.; McKinlay, G.; Smith, W. E. *J. Chem. Soc., Dalton Trans.* **1977**, 1874.(6) Bergerhoff, G. Z. *Anorg. Allg. Chem.* **1964**, *327*, 139.(7) Jackson, H. L.; Makusick, R. C. *Org. Synth.* **1963**, *4*, 438.(8) Esperas, S. *Acta Chem. Scand., Ser. A* **1976**, *A30*, 527.(9) In the secular determinants published previously² values of $+\zeta/2$ and $-\zeta$, respectively, were inadvertently omitted from the diagonal energies of $\Pi_u(^3\Delta_u)$ and $\Sigma_u^+(^3\Pi_u)$; these omissions served only to shift the input $^3\Delta_u$ and $^3\Pi_u$ energies by constant amounts but are corrected in the present calculations.

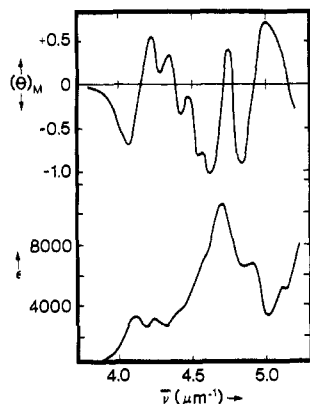


Figure 1. Electronic absorption (lower curve) and MCD (upper curve) spectra of $[\text{Au}(\text{CNEt})_2]\text{ClO}_4$ in acetonitrile solution.

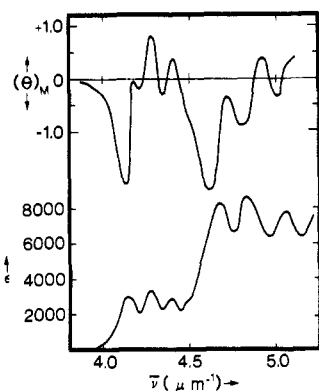


Figure 2. Electronic absorption (lower curve) and MCD (upper curve) spectra of $\text{Au}(\text{CN})(\text{CNMe})$ in acetonitrile solution.

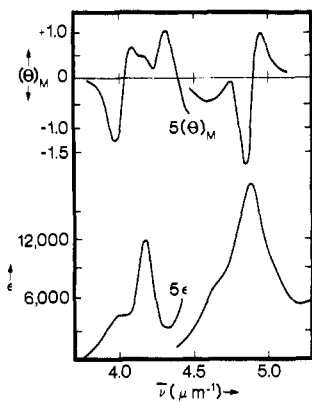


Figure 3. Electronic absorption (lower curves) and MCD (upper curves) spectra of $[\text{Au}(\text{P}(\text{OMe})_3)_2]\text{ClO}_4$ in acetonitrile solution.

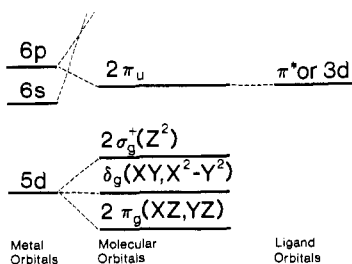


Figure 4. Simplified molecular orbital energy level diagram for linear ($D_{\infty h}$) two-coordinate gold(I) complexes with π -acceptor ligands.

Results and Discussion

Electronic Absorption and MCD Spectra. Figures 1–3 present absorption and MCD spectra for $[\text{Au}(\text{CNEt})_2]^+$, $\text{Au}(\text{CN})(\text{CNMe})$, and $[\text{Au}(\text{P}(\text{OMe})_3)_2]^+$ in acetonitrile solution.

Table I. Electronic Absorption and MCD Spectral Data in Acetonitrile

band no.	absorption		MCD	
	$\bar{\nu}$, μm^{-1}	ϵ , $\text{M}^{-1} \text{cm}^{-1}$	$\bar{\nu}$, μm^{-1}	$[\Theta]_{\text{M}}^c$
$[\text{Au}(\text{CNEt})_2]\text{ClO}_4$				
I	4.12	3300	4.06	-0.71
			4.13	0
			4.20	+0.52
II	4.26	3200	4.30	+0.39
III	4.37	4000 ^a	4.36	-0.30
IV	4.55	6800 ^a	4.55	-0.94
V	4.68	10800	b { 4.60	-1.04
			4.67	0
			4.72	+0.36
VI	4.85	7500	b { 4.80	-1.1
			4.86	0
			4.95	+0.71
VII	5.10	6400	b { 5.06	+0.52 ^a
			5.10	0
$[\text{Au}(\text{CN})(\text{CNMe})]$				
I	4.12	3130	4.11	-1.9
II	4.25	3250	4.22	-0.20
			4.27	+0.83
			4.33	-0.35
III	4.36	2670	4.40	+0.48
IV	4.49	2600 ^a	4.48	-0.9 ^a
V	4.66	8320	4.60	-2.1
VI	4.80	8590	4.77	-0.9
			4.85	0
VII	5.02	7800	4.90	+0.4
			4.97	-0.4
$[\text{Au}(\text{P}(\text{OMe})_3)_2]\text{ClO}_4$				
I	4.00	1050	3.97	-0.28
			4.02	0
			4.05	+0.13
II	4.19	2870	4.16	+0.09 ^a
			4.30	+0.23
III	4.70	8060 ^a	4.62	-0.54
IV	4.92	18200	b { 4.83	-1.90
			4.88	0
			4.93	+0.99
$[(n\text{-C}_4\text{H}_9)_4\text{N}][\text{Au}(\text{CN})_2]$				
I	4.17	4100	4.16	-2.2
			4.20	0
II	4.30	3800	4.30	+0.88
III	4.37	3680	4.39	+0.91
IV	4.53	2640 ^a	4.48	-0.09
			4.53	+0.22
			4.58	-0.20 ^a
V	4.69	8240	b { 4.65	-2.1
			4.68	0
			4.72	+0.13
VI	4.85	12800	b { 4.79	-2.0
			4.87	0
			4.90	+0.77
VII	5.12	15300		

^a Shoulder. ^b A term. ^c $[\Theta]_{\text{M}} = 3300(\Delta A)/(MH)$; ΔA = measured differential absorbance, M = molar concentration, l = path length in cm, H = magnetic field in G.

Detailed spectral data are collected in Table I, which also includes some data for $\text{Au}(\text{CN})_2^-$ for comparison purposes. The spectral patterns exhibited by the three Au(I) complexes studied here show considerable similarity in both absorption and MCD, and in addition there is marked similarity of all three to the spectra of $\text{Au}(\text{CN})_2^-$ reported earlier.^{2,3} The similarity among the spectra argues for an extension of the MLCT assignments of $\text{Au}(\text{CN})_2^-$ to the isocyanide and trimethyl phosphite complexes. Furthermore, the unstable mercury(II) ethyl isocyanide and trimethyl phosphite complexes prepared in our present study, though poorly characterized, showed no absorption shoulders or maxima below 5.2

Table II. MLCT Excited States

confgn ^a	no spin-orbit coupling	spin-orbit states
(2σ _g ⁺)(2π _u)	a ¹ Π _u a ³ Π _u	Π _u Π _u , Σ _u ⁺ , Σ _u ⁻ , Δ _u
(δ _g) ³ (2π _u)	b ¹ Π _u b ³ Π _u	Π _u Π _u , Σ _u ⁺ , Σ _u ⁻ , Δ _u
(2π _g) ³ (2π _u)	¹ φ _u ³ φ _u ¹ Σ _u ⁺ ³ Σ _u ⁺ ¹ Σ _u ⁻ ³ Σ _u ⁻ ¹ Δ _u ³ Δ _u	φ _u φ _u , Δ _u , Γ _u Σ _u ⁺ Σ _u ⁻ , Π _u Σ _u ⁻ Σ _u ⁺ , Π _u Δ _u Δ _u , Π _u , φ _u

^a Filled orbital omitted, ground state = (2π_g)⁴(δ_g)⁴(2σ_g⁺)², ¹Σ_g⁺, Σ_g⁺.

μm⁻¹, indicating a marked blue shift of the corresponding band systems from isoelectronic Au(I) to Hg(II). Such a blue shift is expected from the increased stability of the Hg(II) 5d orbitals over those of Au(I) and is the hallmark of MLCT transitions.

MLCT Excited States. A simplified energy level diagram that will be helpful in visualizing MLCT excited configurations for linear two-coordinate Au(I) complexes is given in Figure 4 (the molecular axis is taken to be the z direction). The ground-state electron configuration is 5d¹⁰ so that the complexes are diamagnetic and have a nondegenerate, totally symmetric ground state, ¹Σ_g⁺. Following the approach used for Au(CN)₂⁻², we interpreted the electronic spectra by a model that involves a single π* orbital in excited configurations, 2π_u, and that allows for gold spin-orbit coupling in the MLCT excited states. The MLCT spin-orbit states that arise from each of the three 5d → 2π_u excited configurations are given in Table II. Only transitions to ¹Σ_u⁺ (z polarized) and ¹Π_u (xy polarized) are fully allowed by dipole selection rules. Therefore to a first approximation only Π_u and Σ_u⁺ spin-orbit states need to be considered, and their wave functions will be given by eq 1 and 2 (a_r-l_i are mixing coefficients from the

$$|\Pi_u(i)\rangle = a_{i1}(a^1\Pi_u) + b_{i1}(a^3\Pi_u) + c_{i1}(^3\Sigma_u^+) + d_{i1}(^3\Delta_u) + e_{i1}(^3\Sigma_u^-) + f_{i1}(b^3\Pi_u) + g_{i1}(b^1\Pi_u) \quad (1)$$

$$|\Sigma_u^+(i)\rangle = h_{i1}(a^3\Pi_u) + j_{i1}(^1\Sigma_u^+) + k_{i1}(^3\Sigma_u^-) + l_{i1}(b^3\Pi_u) \quad (2)$$

spin-orbit eigenvectors; the singlet and triplet states are those expected in the absence of spin-orbit coupling).²

MCD A and B Terms.^{10,11} The MCD for diamagnetic Au(I) complexes will consist of A₁ terms for Π_u excited states and B₀ terms for both Σ_u⁺ and Π_u excited states. The A₁ terms for each Π_u state are given by eq 3,¹¹ where L_z and S_z are

$$A_1(j) = i/2\langle\Pi_u(j)|x|L_z + 2S_z|\Pi_u(j)y\rangle|D_0(^1\Pi_u)|^2 \quad (3)$$

orbital and spin angular momentum operators in the z direction and |D₀(¹Π_u)|² = |⟨¹Σ_g⁺||m_x||¹Π_u⟩|², the dipole strength of the fully allowed ¹Σ_g⁺ → ¹Π_u transition. With use of the spin-orbit wave function of eq 1, the expression for A₁(j) becomes eq 4.

$$A_1(j) = \frac{1}{2}[(|a_j|^2 - |b_j|^2 - 2|c_j|^2 + 2|e_j|^2 - |f_j|^2 + |g_j|^2)[|a_j|^2|D_0(a^1\Pi_u)|^2 + |g_j|^2|D_0(b^1\Pi_u)|^2] \quad (4)$$

The B₀ term for a transition a → j requires a summation over all states k ≠ j, as given by eq 5,¹¹ but because of the inverse

$$B_0(a \rightarrow j) = -(2i/3)\sum(W_k - W_j)^{-1}\langle j|L + 2S|k\rangle\langle a|m_j\rangle x\langle k|m_a\rangle \quad (5)$$

dependence on the energy difference between the states k and j, (W_k - W_j)⁻¹, the states k closest in energy to j will make the greatest contribution to B₀(a → j). Thus for a MLCT transition in the UV region, the summation can be truncated to a good approximation to include only the other MLCT excited states. The B₀ terms can then be written as

$$B_0[\Pi_u(j)] = \sum_k B_0(\Pi_u, \Pi_u)_{jk} + \sum_k B_0(\Pi_u, \Sigma_u^+)_{jk}$$

and

$$B_0[\Sigma_u^+(j)] = \sum_k B_0(\Sigma_u^+, \Pi_u)_{jk}$$

where k ranges over all the Σ_u⁺(i) and Π_u(i) MLCT states and B₀(Π_u, Π_u)_{jk} and B₀(Σ_u⁺, Π_u)_{jk} are given by eq 6 and 7. In

$$B_0(\Pi_u, \Pi_u)_{jk} = -(W_k - W_j)^{-1}[a_j^*a_k - b_j^*b_k - 2c_j^*c_k + 2e_j^*e_k - f_j^*f_k + g_j^*g_k][a_k^*a_j|D_0(a^1\Pi_u)|^2 + g_k^*g_j|D_0(b^1\Pi_u)|^2] \quad (6)$$

$$B_0(\Sigma_u^+, \Pi_u)_{jk} = -(W_k - W_j)^{-1}[2^{1/2}h_j^*a_k + (\frac{3}{2})^{1/2}j_j^*a_k - 2^{1/2}ih_j^*b_k - \frac{3}{2}k_j^*b_k + 2j_j^*c_k + (\frac{3}{2})^{1/2}h_j^*c_k + 2^{-1/2}l_j^*c_k + (\frac{3}{2})^{1/2}h_j^*d_k - (\frac{3}{2})^{1/2}h_j^*e_k - 2k_j^*e_k - 2^{-1/2}l_j^*e_k + k_j^*f_k - 2^{-1/2}il_j^*f_k - j_j^*g_k - 2^{-1/2}l_j^*g_k][j_j^*a_k^*(D_0(^1\Sigma_u^+)) \times (D_0^*(a^1\Pi_u x)) + j_j^*g_k^*(D_0(^1\Sigma_u^+))(D_0^*(b^1\Pi_u x))] \quad (7)$$

eq 6 and 7, D₀(¹Σ_u⁺) = 3^{1/2}⟨¹Σ_g⁺||m_x||¹Σ_u⁺⟩, D₀^{*}(a¹Π_ux) = 3^{1/2}⟨¹Σ_g⁺||m_x||a¹Π_ux⟩*, and D₀^{*}(b¹Π_ux) = 3^{1/2}⟨¹Σ_g⁺||m_x||b¹Π_ux⟩* and use is made of the relations B₀(Π_u, Π_u)_{kj} = -B₀(Π_u, Π_u)_{jk} and B₀(Π_u, Σ_u⁺)_{kj} = -B₀(Σ_u⁺, Π_u)_{jk}.

Interpretation of the Au(CNet)₂⁺ Spectra. A comparison of Figure 1 with the spectra of Au(CN)₂⁻ (Table II and ref 2 and 3) suggests some parallel MLCT assignments. The two intense absorption bands for Au(CNet)₂⁺ at 4.68 (band V) and 4.85 μm⁻¹ (band VI) have positive A terms associated with them in the MCD, similar to corresponding bands Au(CN)₂⁻ at 4.69 and 4.85 μm⁻¹, respectively. Logically these bands are assigned to spin-orbit states composed principally of the singlet states a¹Π_u and b¹Π_u, respectively. Both of these states are predicted to have positive A terms in agreement with experiment. Band V at 4.69 μm⁻¹ observed for Au(CN)₂⁻ has also been shown to be xy polarized,² which further supports the Π_u assignment.

The lower intensity bands below 4.6 μm⁻¹ (bands I-IV) present some difficulty in interpretation. For example the MCD associated with band I suggests a large positive A term. The assignment for band I of Au(CN)₂⁻ based on polarization studies was to the Σ_u⁺(a³Π_u) and Π_u(a³Π_u) spin-orbit states at nearly the same energy.² At first glance neither of these states is consistent with the observed MCD for Au(CNet)₂⁺ (or Au(CN)₂⁻) because Π_u(a³Π_u) should exhibit a negative A term and Σ_u⁺ should not show any A term. Indeed if the previous assignments of Au(CN)₂⁻ are followed, there should be no positive A terms lower in energy than band V. If the Au(CN)₂⁻ assignments are applicable, the large MCD associated with band I of Au(CNet)₂⁺ must be assigned as a pseudo A term¹⁰ resulting from overlapping B terms of opposite sign from two states lying close in energy. In order to test this possibility and to provide a basis for interpreting the remainder of the MCD spectrum for Au(CNet)₂⁺, we performed some calculations of A₁ and B₀ terms. These calculations are necessarily crude because of the approximations that must be made in determining the spin-orbit MLCT wave functions and the D₀ integrals in eq 4, 6 and 7. These latter integrals are difficult to calculate exactly since they involve orbitals over

(10) For a review of MCD spectroscopy see: Stephens, P. J. *Annu. Rev. Phys. Chem.* 1974, 25, 201 and references cited therein.

(11) Stephens, P. J. *Adv. Chem. Phys.* 1976, 35, 197. The MCD conventions set forth in this paper are used here throughout.

Table III. Calculated Spin-Orbit Energies and Mixing Coefficients

state	energy, μm^{-1}	$a^1\Pi_u$	$a^3\Pi_u$	$^3\Sigma_u^+$	$^3\Delta_u$	$^3\Sigma_u^-$	$b^3\Pi_u$	$b^1\Pi_u$
$\Pi_u(1)$	4.138	-0.031	0.958 <i>i</i>	-0.095	0.133	-0.218	0.076 <i>i</i>	0.005
$\Pi_u(2)$	4.260	-0.018	-0.939 <i>i</i>	0.092	-0.017	-0.129	0.926 <i>i</i>	0.326
$\Pi_u(3)$	4.681	0.745	0.125 <i>i</i>	-0.011	0.178	0.566	0.014 <i>i</i>	0.275
$\Pi_u(4)$	4.851	-0.543	0.069 <i>i</i>	-0.377	-0.112	0.449	-0.108 <i>i</i>	0.575
$\Pi_u(5)$	5.298	-0.231	0.114 <i>i</i>	-0.018	-0.046	0.612	0.329 <i>i</i>	-0.669
$\Pi_u(6)$	5.755	-0.208	0.148 <i>i</i>	0.915	-0.081	0.194	-0.123 <i>i</i>	0.195
$\Pi_u(7)$	6.046	-0.226	-0.131 <i>i</i>	0.049	0.964	0.021	-0.003 <i>i</i>	0.005

state	energy, μm^{-1}	$a^3\Pi_u$	$^1\Sigma_u^+$	$^3\Sigma_u^-$	$b^3\Pi_u$	state	energy, μm^{-1}	$a^3\Pi_u$	$^1\Sigma_u^+$	$^3\Sigma_u^-$	$b^3\Pi_u$
$\Sigma_u^+(1)$	4.127	0.946	0.094	0.299 <i>i</i>	0.076	$\Sigma_u^+(3)$	5.125	-0.222	-0.088	0.849 <i>i</i>	-0.470
$\Sigma_u^+(2)$	4.555	-0.188	-0.190	0.415 <i>i</i>	0.871	$\Sigma_u^+(4)$	6.185	-0.147	0.973	0.128 <i>i</i>	0.121

Table IV. Calculated MCD Terms for each MLCT Spin-Orbit State for $\text{Au}(\text{CNET})_2^+$

state	$\bar{\nu}(\text{calcd}),$ μm^{-1}	A_1 term ^a	B_0 term	
			$\Sigma B_0(\Pi_u, \Pi_u)^a$	$\Sigma B_0(\Pi_u, \Sigma_u^+)^b$
$\Sigma_u^+(1)$	4.127			
$\Pi_u(1)$	4.139	-8.3×10^{-4}	-7.9×10^{-7}	-1.72×10^{-1}
$\Pi_u(2)$	4.260	-8.0×10^{-2}	-2.1×10^{-5}	-1.15×10^{-4}
$\Sigma_u^+(2)$	4.555			$+1.50 \times 10^{-3}$
$\Pi_u(3)$	4.680	$+7.9 \times 10^{-1}$	$+5.4 \times 10^{-5}$	-5.3×10^{-4}
$\Pi_u(4)$	4.851	$+4.6 \times 10^{-1}$	-3.9×10^{-5}	-3.3×10^{-4}
$\Sigma_u^+(3)$	5.125			$+3.7 \times 10^{-4}$
$\Pi_u(5)$	5.299	$+5.7 \times 10^{-1}$	-1.92×10^{-5}	-3.9×10^{-4}
$\Pi_u(6)$	5.755	-1.27×10^{-1}	$+2.17 \times 10^{-5}$	-3.8×10^{-4}
$\Pi_u(7)$	6.046	$+1.52 \times 10^{-3}$	$+3.9 \times 10^{-6}$	$+2.05 \times 10^{-4}$
$\Sigma_u^+(4)$	6.185			-8.5×10^{-6}

^a Dipole factor $|D_0(a^1\Pi_u)|^2 = |D_0(b^1\Pi_u)|^2$. ^b Dipole factor $|D_0(^1\Sigma_u^+)|D_0(a^1\Pi_u)| = |D_0(^1\Sigma_u^+)|D_0(b^1\Pi_u)|$.

more than one atomic center. However, the numerical sign of the integrals can be deduced by approximating the metal-centered orbitals as pure 5d functions and the $2\Pi_u$ MO's as 2p orbitals on carbon. For example, $D_0(^1\Sigma_u^+) \approx \langle (-d_{zz})|m_z|(p_x) \rangle$. The squared quantities $|D_0|^2$ will be positive, while considerations of orbital overlap predict $D_0(^1\Sigma_u^+)$ and $D_0(a^1\Pi_u)$ to be negative and $D_0(b^1\Pi_u)$ to be positive with our choice of phase.¹² We further arbitrarily take the magnitudes $|D_0(a^1\Pi_u)|$ and $|D_0(b^1\Pi_u)|$ to be the same. Consequently the calculated A_1 and B_0 terms are valid only as approximate relative measures of the MCD terms, but the calculated terms should at least be able to predict the sign of the observed MCD. The calculations begin with the determination of spin-orbit energies and mixing coefficients from the spin-orbit eigenvectors (see Experimental Section for details), which are presented in Table III. The mixing coefficients were then used in eq 4, 6, and 7 to calculate the A_1 and B_0 terms for each spin-orbit MLCT state; these calculated terms are summarized in Table IV. It should be noted that since the $B_0(\Pi_u, \Pi_u)_{jk}$ quantities contain different dipole factors than the $B_0(\Sigma_u^+, \Pi_u)_{jk}$, the two types of sums cannot be combined directly. However, if the dipole factors are similar in magnitude as they are expected to be, then the $B_0(\Sigma_u^+, \Pi_u)$ contributions consistently dominate the B_0 terms. The calculated MLCT energies are compared with the experimentally observed spectral bands of $\text{Au}(\text{CNET})_2^+$ in Figure 5.

The agreement between the calculated MCD terms (Table IV) and the experimental spectra (Table II) for $\text{Au}(\text{CNET})_2^+$ is remarkably good considering the approximations involved. The results show that the interpretation of the lowest energy feature in the MCD spectrum as a pseudo A term developed from the close proximity of the $\Sigma_u^+(1)$ and $\Pi_u(1)$ states ($\Sigma_u^+(a^3\Pi_u)$ and $\Pi_u(a^3\Pi_u)$, respectively) is feasible. The

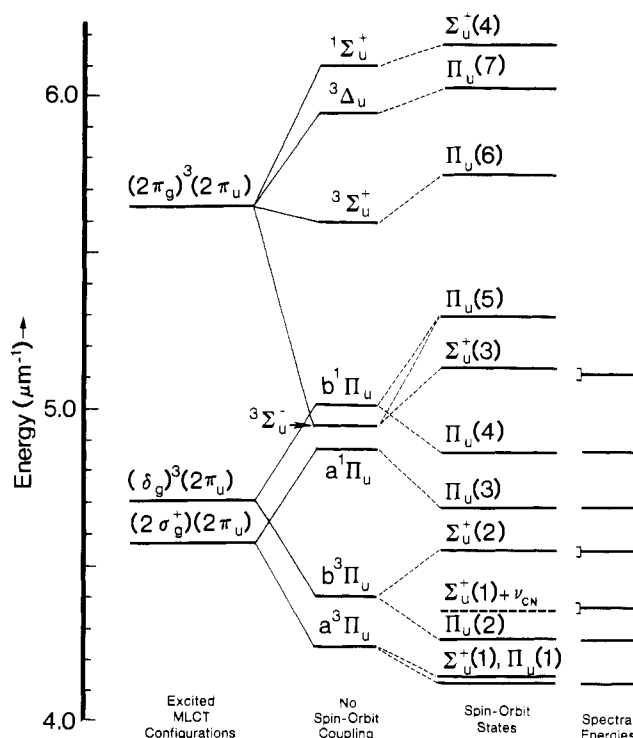


Figure 5. Comparison between the calculated spin-orbit MLCT states for $\text{Au}(\text{CNET})_2^+$ and the observed spectral bands. Input parameters for the calculated states (in μm^{-1}) are as follows: $\zeta = 0.30$; $a^1\Pi_u = 4.88$, $a^3\Pi_u = 4.24$, $^3\Sigma_u^+ = 5.60$, $^1\Sigma_u^+ = 6.10$, $^3\Delta_u = 5.80$, $^3\Sigma_u^- = 4.96$, $b^3\Pi_u = 4.40$, $b^1\Pi_u = 5.01$.

close-lying bands of opposite polarization observed² in the region of band I for $\text{Au}(\text{CN})_2^-$ is compatible with the present results also and offers further support for the interpretation.

The assignment of band II for $\text{Au}(\text{CNET})_2^+$ at $4.26 \mu\text{m}^{-1}$ is to $\Pi_u(2)$; the MCD should show a negative A_1 term and a negative B_0 term. The observed MCD exhibits a "dip" at the maximum of band II even though it is positive at all energies in this region. The generally positive MCD is likely a result of the close proximity of the positive portion of the large pseudo A term at lower energy. The "dip" in the spectrum is interpreted as smaller negative A_1 and B_0 terms superimposed on the larger positive portion of the pseudo A term of band I.

The spectra for $\text{Au}(\text{CNET})_2^+$ from 4.2 to $4.6 \mu\text{m}^{-1}$ is not clearly resolved, and the intense band V partially obscures this region. There are at least two shoulders at 4.37 and $4.55 \mu\text{m}^{-1}$. The lower energy shoulder is not accounted for in the spin-orbit calculation and is tentatively assigned to an excited-state C-N stretching vibration built on the $\Sigma_u^+(1)$ origin. The MCD shows a negative B_0 term for this band, which is consistent with this assignment. The shoulder at $4.55 \mu\text{m}^{-1}$ is assigned to $\Sigma_u^+(2)$. The predicted positive B_0 term for this

(12) Griffith, J. S. "The Theory of Transition Metal Ions"; Cambridge University Press: London, 1964.

state is likely responsible for the smaller shoulder on the low-energy side of the much larger negative portion of the positive A term associated with the intense band V. Higher resolution spectra are needed to clarify the assignments in the 4.2–4.6- μm^{-1} region.

The assignment of bands V and VI to $\Pi_u(3)$ and $\Pi_u(4)$, respectively, is supported by the calculated positive A_1 terms. The observed MCD shows clearly two positive A terms that overlap slightly. The same pattern is observed³ for $\text{Au}(\text{CN})_2^-$, though band VI is more intense than band V—just the reverse of that observed for $\text{Au}(\text{CNET})_2^+$.

The highest energy band observed for $\text{Au}(\text{CNET})_2^+$ at 5.1 μm^{-1} (band VII) is likely due to $\Sigma_u^+(3)$ or a combination of $\Sigma_u^+(3)$ and $\Pi_u(5)$. The MCD in this region shows a poorly resolved positive shoulder and then passes through zero near the band's maximum, but it must be noted that the signal-to-noise ratio in the MCD at this high energy was not very favorable. The calculations show a positive A_1 term is expected for $\Pi_u(5)$ but a negative pseudo A term is expected from the combination of $\Sigma_u^+(3)$ and $\Pi_u(5)$. The experimental MCD is simply not adequate to differentiate between these two predictions or combinations thereof.

Au(CN)(CNMe) and Au[P(OMe)₃]₂⁺ Spectra. The absorption and MCD spectra of $\text{Au}(\text{CN})(\text{CNMe})$ parallel those of $\text{Au}(\text{CNET})_2^+$ and $\text{Au}(\text{CN})_2^-$ to a high degree in both energy and band pattern. Thus common MLCT assignments are indicated. There is no evidence in the spectra for separate MLCT transitions to the CN^- and CNMe ligands. Consequently, the ligand π^* -acceptor levels must be close in energy. Similar observations have been made for MLCT in mixed CN^- - CNR complexes of $\text{Pt}(\text{II})$.¹³ The MCD in the region of band I for $\text{Au}(\text{CN})(\text{CNMe})$ appears to show the characteristics of the B -term components more clearly than band I for $\text{Au}(\text{CNET})_2^+$. The spectrum in this region in many respects is reflective of the MCD observed for $\text{Au}(\text{CN})_2^-$ (see Table I and ref 3), where the pseudo A term is also fairly unsymmetrical. The unsymmetrical appearance of the MCD terms for $\text{Au}(\text{CN})(\text{CNMe})$ and $\text{Au}(\text{CN})_2^-$ may be a direct result of a larger separation and slightly different composition of the $\Sigma^+(1)$ and $\Pi(1)$ states compared to those of $\text{Au}(\text{CNET})_2^+$. The MCD is expected to be sensitive to small changes in energy and relative magnitude of the spin-orbit mixing coefficients, so that distortion of the nearly derivative-shaped pseudo A term would not be surprising.

The spectra for $\text{Au}[\text{P}(\text{OMe})_3]_2^+$ are less well resolved than for $\text{Au}(\text{CNET})_2^+$, but the intense band at 4.92 μm^{-1} and shoulder at 4.70 μm^{-1} parallel the intense bands for $\text{Au}(\text{CNET})_2^+$ and $\text{Au}(\text{CN})_2^-$ observed in this region. Thus the assignment of $\Pi_u(a^1\Pi_u)$ and $\Pi_u(b^1\Pi_u)$ to bands III and IV, respectively, for $\text{Au}[\text{P}(\text{OMe})_3]_2^+$ follows by analogy to $\text{Au}(\text{CNET})_2^+$ or $\text{Au}(\text{CN})_2^-$. The lower energy region 3.9–4.5 μm^{-1} appears qualitatively different in the absorption spectrum, exhibiting only two features with band I weaker than the very prominent band II. The MCD does show the pseudo A term for band I and a pronounced "dip" near the band maximum of band II, reminiscent of the MCD for band II for $\text{Au}(\text{CNET})_2^+$. The spectra in this region are expected to be different because of the absence of the vibrational component involving ν_{CN} (band III for $\text{Au}(\text{CNET})_2^+$ or $\text{Au}(\text{CN})(\text{CNMe})$).

The reason for the enhanced intensity of band II is not clear but may be related to relocation of the $\Sigma_u^+(2)$ state to lower energy. This state is predicted to have a substantial positive B_0 term and may be responsible for the prominent positive MCD at 4.30 μm^{-1} . Further details about the lower energy region must await higher resolution spectra.

Electronic Structure of π -Acceptor Au(I) Complexes. The input parameters used to calculate the MLCT spin-orbit states and MCD terms for $\text{Au}(\text{CNET})_2^+$ (see Figure 5) can be used to estimate the relative energies of the excited MLCT configurations, if it is assumed that electron repulsion differences are small. The parameters lead to the ordering of the occupied 5d MO levels of Au(I) as $2\sigma_g^+(z^2) > \delta_g(xy, x^2 - y^2) > 2\pi_g^-(xz, yz)$. The similarity in band positions between $\text{Au}(\text{CNET})_2^+$ and $\text{Au}(\text{CN})(\text{CNMe})$ or $\text{Au}[\text{P}(\text{OMe})_3]_2^+$ indicates the same energy ordering is applicable. The stability of the $2\pi_g^-(xz, yz)$ level relative to the strictly nonbonding $\delta_g(xy, x^2 - y^2)$ level implies Au(I) 5d to ligand π back-bonding. However, it should be noted that the exact placement of the $2\pi_g^-(xz, yz)$ level below the $\delta_g(xy, x^2 - y^2)$ level is uncertain because only one of the MLCT states of the $(2\pi_g^+)^3(2\pi_u)$ configuration can be observed in the experimental spectra; the rest were calculated to be too high in energy. The best calculations consistently placed the $2\pi_g^-(xz, yz) \sim 0.9 \mu\text{m}^{-1}$ lower in energy than $\delta_g(xy, x^2 - y^2)$. This stabilization is larger than inferred for $\text{Au}(\text{CN})_2^-$ ($\sim 0.3 \mu\text{m}^{-1}$)² but would be consistent with better π -acceptor ability of the neutral CNR (and $\text{P}(\text{OMe})_3$ also) ligands than the anionic CN^- .

The participation of the $5d_{z^2}$ orbital of Au(I) in σ bonding can be inferred by comparison of the weakly antibonding $2\sigma_g^+(z^2)$ level with the nonbonding $\delta_g(xy, x^2 - y^2)$ level. The participation must be small since the separation between these two levels is only $\sim 0.14 \mu\text{m}^{-1}$. This result compares with that for $\text{Au}(\text{CN})_2^-$, where the separation was not measurable,² and with studies on AuX_2^- ($X = \text{Cl}^-, \text{Br}^-, \text{I}^-$) ions,¹ where the separation was 0.2–0.3 μm^{-1} . Consequently the strength of σ bonding in these Au(I) complexes must rely on orbitals other than the Au(I) $5d_{z^2}$ —likely 6s and 6p_z as sp_z hybrids on the Au(I) ion. Thus the notion advanced by Orgel¹⁴ and cited in textbooks¹⁵ that d_{z²} hybridization is responsible for σ bonding in linear two-coordinate complexes is probably not correct for Au(I). Rather sp hybridization of Au(I) is more reasonable. This conclusion has also been advanced from Au-197 Mössbauer studies of a variety of two-coordinate Au(I) complexes.^{16–19}

Acknowledgment is made to the donors of the Petroleum Research Fund, administered by the American Chemical Society, for the support of this research.

Registry No. $[\text{Au}(\text{CNET})_2]\text{ClO}_4$, 82582-20-5; $\text{Au}(\text{CN})(\text{CNMe})$, 60974-76-7; $[\text{Au}(\text{P}(\text{OMe})_3)_2]\text{ClO}_4$, 82598-60-5.

(13) Isci, H.; Mason, W. R. *Inorg. Chem.* **1975**, *14*, 913.

(14) Orgel, L. E. *J. Chem. Soc.* **1958**, 4186. Dunitz, J. D.; Orgel, L. E. *Adv. Inorg. Chem. Radiochem.* **1960**, *2*, 1.

(15) See for example: Cotton, F. A.; Wilkinson, G. "Advanced Inorganic Chemistry", 4th ed.; Wiley-Interscience: New York, 1980; p 969. Huheey, J. E. "Inorganic Chemistry", 2nd ed.; Harper and Row: New York, 1978; p 426.

(16) Faltens, M. O.; Shirley, D. A. *J. Chem. Phys.* **1970**, *53*, 4249.

(17) Charlton, J. S.; Nichols, D. I. *J. Chem. Soc. A* **1970**, 1484.

(18) McAuliffe, C. A.; Parish, R. V.; Randall, P. D. *J. Chem. Soc., Dalton Trans.* **1977**, 1426.

(19) Jones, P. G.; Maddock, A. G.; Mays, M. J.; Mair, M. M.; Williams, A. F. *J. Chem. Soc., Dalton Trans.* **1977**, 1934.